

## Specific Interactions of Complementary Mono- and Multivalent Guests with Recognition-Induced Polymersomes

Raymond J. Thibault Jr., Trent H. Galow, Erik J. Turnberg, Mark Gray,  
Peter J. Hotchkiss, and Vincent M. Rotello\*

Contribution from the Department of Chemistry, University of Massachusetts,  
Amherst, Massachusetts 01003

Received April 4, 2002

**Abstract:** We have explored the interactions of mono- and multivalent guests with Recognition-Induced Polymersomes (RIPs) formed from complementary random copolymers featuring diamidopyridine and thymine functionality. Addition of monovalent guests featuring imide functionality to these RIPs induced a temporary swelling of the vesicles, followed by dissociation of the vesicles due to competitive binding of the guest. Conversely, multivalent thymine-functionalized nanoparticle guests were rapidly incorporated into the RIPs, inducing a contraction of RIP diameter over time. These mono- and multivalent interactions were extremely specific: highly analogous control systems showed no interaction with the RIP structures. Taken together, these studies demonstrate highly selective molecular “lock and key” control over higher-order assembly and recognition processes.

### Introduction

The closed bilayer structure of vesicular systems provides a versatile tool for a variety of applications. As formed, these systems are used as cell models,<sup>1</sup> biosensors,<sup>2</sup> and encapsulating agents for drug delivery.<sup>3</sup> Vesicular architectures also furnish effective templates for the controlled construction of functional materials ranging from nano- to micrometer dimensions. The ability to finely control composition, morphology, and function of vesicles allows for the formation of novel templated materials with a diversity of function, including organic capsules,<sup>4</sup> inorganic capsules,<sup>5</sup> and biological models.<sup>6</sup>

Specific molecular recognition processes<sup>7</sup> provide a tool for obtaining molecular-level control over higher-order assembly

processes.<sup>8</sup> Integration of the “lock and key” selectivity inherent in molecular recognition with the phase-separated characteristics and 3-D nature of vesicular templates<sup>9</sup> presents a new opportunity for the creation of highly structured constructs featuring new structural and dynamic properties. In recent studies,<sup>10</sup> we reported that complementary random copolymers **1** and **2** (Figure 1) spontaneously self-assemble in nonaqueous media to form giant vesicles (Figure 2).<sup>11</sup> Unlike previously reported diblock copolymer-based polymersomes that rely upon phase segregation for self-assembly,<sup>12,13</sup> these Recognition-Induced Polymersomes (RIPs) are formed through highly specific interactions between the complementary random co-

\* To whom correspondence should be addressed. E-mail: rotello@chem.umass.edu.

- (1) Paleos, C. M.; Sideratou, Z.; Tsiourvas, D. *ChemBiochem* **2001**, *2*, 305–310.
- (2) Okada, S.; Peng, S.; Spevak, W.; Charych, D. *Acc. Chem. Res.* **1998**, *31*, 229–239. Braguglia, C. M. *Chem. Biochem. Eng. Q.* **1998**, *12*, 183–190. Stelzle, M.; Weissmüller, G.; Sackmann, E. *J. Phys. Chem.* **1993**, *97*, 2974–2981. Jelinek, R.; Kolusheva, S. *Biotechnol. Adv.* **2001**, *19*, 109–118. Taylor, M. A.; Jones, M. N.; Vadgama, P. M.; Higson, S. P. *J. Biosens. Bioelectron.* **1995**, *10*, 251–260.
- (3) Zasadzinski, J. A. *Curr. Opin. Solid State Mater. Sci.* **1997**, *2*, 345–349. Uchegbu, I. F.; Vyas, S. P. *Int. J. Pharm.* **1998**, *172*, 33–70. Brown, M. D.; Schatzlein, A.; Brownlie, A.; Jack, V.; Wang, W.; Tetley, L.; Gray, A. I.; Uchegbu, I. F. *Bioconjugate Chem.* **2000**, *11*, 880–891. Hafez, I. M.; Cullis, P. R. *Adv. Drug Deliv. Rev.* **2001**, *47*, 139–148.
- (4) Menger, F. M.; Caran, K. L.; Apkarian, R. P. *Langmuir* **2000**, *16*, 98–101. Menger, F. M.; Angelova, M. I. *Acc. Chem. Res.* **1998**, *31*, 789–797. Caruso, F. *Chem.-Eur. J.* **2000**, *6*, 413–419. Holmlin, R. E.; Schiavoni, M.; Chen, C. Y.; Smith, S. P.; Prentiss, M. G.; Whitesides, G. M. *Angew. Chem., Int. Ed.* **2000**, *39*, 3503–+. Nardin, C.; Hirt, T.; Leukel, J.; Meier, W. *Langmuir* **2000**, *16*, 1035–1041. Dobereiner, H. G. *Curr. Opin. Coll. Interface Sci.* **2000**, *5*, 256–263. Luo, L. B.; Eisenberg, A. *J. Am. Chem. Soc.* **2001**, *123*, 1012–1013.
- (5) Antonelli, D. M. *Microporous Mesoporous Mater.* **1999**, *33*, 209–214. Jung, J. H.; Ono, Y.; Sakurai, K.; Sano, M.; Shinkai, S. *J. Am. Chem. Soc.* **2000**, *122*, 8648–8653. Hubert, D. H. W.; Jung, M.; Frederik, P. M.; Bomans, P. H. H.; Meuldijk, J.; German, A. L. *Adv. Mater.* **2000**, *12*, 1286–+. Hubert, D. H. W.; Jung, M.; German, A. L. *Adv. Mater.* **2000**, *12*, 1291–+.
- (6) Oliver, S.; Kuperman, A.; Coombs, N.; Lough, A.; Ozin, G. A. *Nature* **1995**, *378*, 47–50.
- (7) For a comprehensive recent review, see: Prins, L. J.; Reinhoudt, D. N.; Timmerman, P. *Angew. Chem., Int. Ed.* **2001**, *40*, 2383–2426.
- (8) Taton, T. A.; Mirkin, C. A.; Letsinger, R. L. *Science* **2000**, *289*, 1757–1760. Chen, K. M.; Jiang, X. P.; Kimerling, L. C.; Hammond, P. T. *Langmuir* **2000**, *16*, 7825–7834. Galow, T. H.; Boal, A. K.; Rotello, V. M. *Adv. Mater.* **2000**, *12*, 576–579. Archer, E. A.; Goldberg, N. T.; Lynch, V.; Krische, M. J. *J. Am. Chem. Soc.* **2000**, *122*, 5006–5007.
- (9) For recent publications on a range of vesicular systems, see: Jones, M. N. *Curr. Opin. Coll. Interface Sci.* **1996**, *1*, 91–100. Engberts, J.; Kevelam, J. *Curr. Opin. Coll. Interface Sci.* **1996**, *1*, 779–789. Lasic, D. D. *Angew. Chem.-Int. Edit. Engl.* **1994**, *33*, 1685–1698. Zasadzinski, J. A.; Kisak, E.; Evans, C. *Curr. Opin. Coll. Interface Sci.* **2001**, *6*, 85–90. Cevc, G.; Richardsen, H. *Adv. Drug Deliv. Rev.* **1999**, *38*, 207–232. Scrimin, P.; Tecilla, P. *Curr. Opin. Chem. Biol.* **1999**, *3*, 730–735. Uchegbu, I. F.; Vyas, S. P. *Int. J. Pharm.* **1998**, *172*, 33–70.
- (10) Ilhan, F.; Galow, T. H.; Gray, M.; Clavier, G.; Rotello, V. M. *J. Am. Chem. Soc.* **2000**, *122*, 5895–5896.
- (11) Marchi-Artzner, V.; Lehn, J. M.; Kunitake, T. *Langmuir* **1998**, *14*, 6470–6478. Wick, R.; Walde, P.; Luisi, P. L. *J. Am. Chem. Soc.* **1995**, *117*, 1435–1436. Luisi, P. L.; Walde, P.; Oberholzer, T. *Curr. Opin. Coll. Interface Sci.* **1999**, *4*, 33–39. Seifert, U. *Mol. Cryst. Liq. Cryst. Sci. Technol. Sect. A—Mol. Cryst. Liq. Cryst.* **1997**, *292*, 213–225.
- (12) Discher, B. M.; Hammer, D. A.; Bates, F. S.; Discher, D. E. *Curr. Opin. Coll. Interface Sci.* **2000**, *5*, 125–131. Hotz, J.; Meier, W. *Langmuir* **1998**, *14*, 1031–1036.
- (13) Discher, B. M.; Won, Y. Y.; Ege, D. S.; Lee, J. C. M.; Bates, F. S.; Discher, D. E.; Hammer, D. A. *Science* **1999**, *284*, 1143–1146. Lee, J. C. M.; Bermudez, H.; Discher, B. M.; Sheehan, M. A.; Won, Y. Y.; Bates, F. S.; Discher, D. E. *Biotechnol. Bioeng.* **2001**, *73*, 135–145.

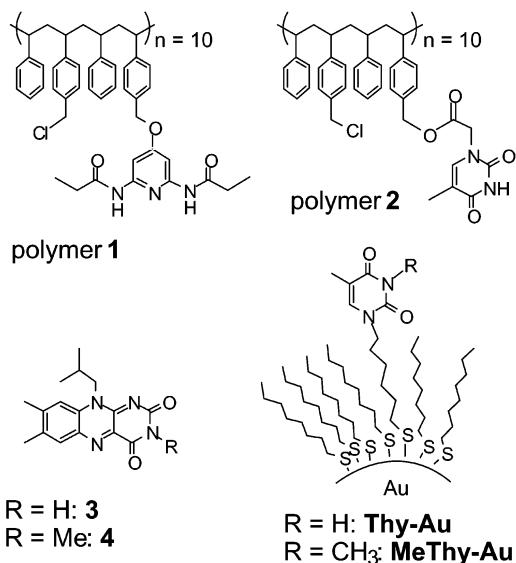


**Figure 1.** Diacyldiaminopyridine- and thymine-based random copolymers **1** and **2**, flavin **3**, N(3)-methyl flavin **4**, and nanoparticles **Thy-Au**, and **MeThy-Au**, featuring 1:9 thymine/octanethiol substitution.

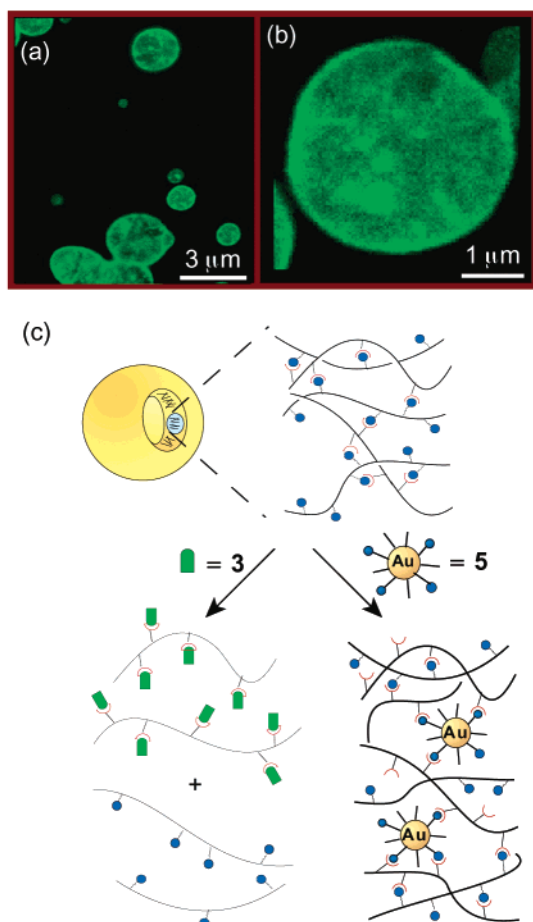


**Figure 2.** (a) Laser Confocal Scanning (LCS) Micrograph of RIPs demonstrating vesicular structure, (b) magnified LCS image,<sup>10</sup> (c) Schematic representation of the effects of incorporation of complementary molecules into RIPs have on polymer strands. Flavin competitively disrupts the hydrogen bonds holding polymers **1** and **2** together while **Thy-Au** inserts into the polymer network, further cross-linking the polymer strands together.

polymer chains. This mode of assembly provides a new tool for the control of vesicle structure; complementary monovalent

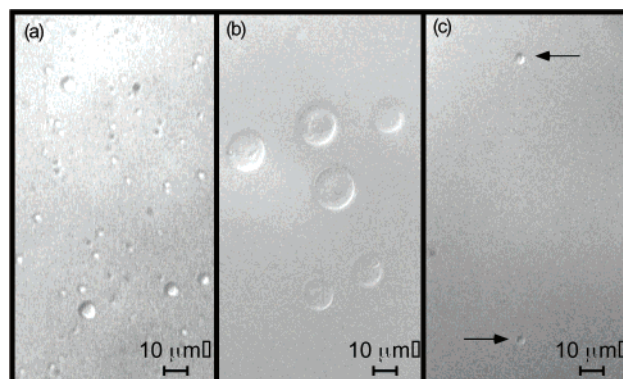


**Figure 3.** DIC micrographs (40 $\times$  magnification) of (a) RIPs before introduction of flavin **3**, (b) 30 s, and (c) 40 min after addition of **3**, for a DAP:**3** ratio of 12:1 (RIPs are indicated by arrows).

and multivalent guests would be expected to distort or disrupt vesicle structure through competitive binding to the polymer recognition sites. Additionally, at lower guest concentrations, RIPs would provide specificity in guest uptake, with favorable enthalpic interactions between the complementary guest and polymer chains compensating for the loss of translational entropy that occurs upon guest incorporation. To test these hypotheses, we have studied the interactions of RIPs with mono- and multivalent guests. We report here the specific interaction of monovalent guest flavin **3**<sup>14</sup> and multivalent nanoparticle **Thy-Au** with RIPs formed from polymers **1** and **2**.

## Results and Discussion

Our initial investigations explored the interaction of flavin **3** with RIPs formed from polymers **1** and **2**. In these experiments, monovalent imide guest **3** was added to preformed RIPs, and the changes in RIP size and number were quantified using time-lapse Differential Interference Contrast (DIC) microscopy studies (Figure 3). Three different flavin **3** to diamidopyridine (DAP, on polymer **1**) molar ratios were investigated over a 50 min period. At the highest concentration of **3**, a 1:1 ratio of DAP:**3**, an initial increase in RIP size was followed by an almost immediate disruption of the vesicle structure (Figure 4). At the lower concentrations of **3**, 12:1 and 2.5:1 DAP:**3**, there was likewise a short-lived increase in average RIP diameter. Complete disruption of structure occurred after 40 min at 2.5:1 ratios of DAP:**3**, whereas at 12:1 ratios, a period of slow contraction occurred providing a RIP size essentially identical to the initial vesicles. The resulting size distribution at this flavin level corresponds reasonably well with the standard probability function<sup>15,16</sup> observed prior to the addition of **3** (Figure 5), suggesting that this is the preferred equilibrium size for the vesicles. An overall decrease in the number of vesicles in solution was concurrent with RIP contraction at the 12:1 molar ratios. No change in vesicle size or concentration occurred with the analogous control flavin **4**, demonstrating that specific recognition is required for the morphological effects observed.

A proposed mechanism for the observed RIP behavior is shown in Figure 6. Upon addition of **3** to the RIP, the imide

(14) Niemz, A.; Rotello, V. M. *Acc. Chem. Res.* **1999**, *32*, 44–52.

(15) Mavelli, F.; Luisi, P. L. *J. Phys. Chem.* **1996**, *100*, 16 600–16 607.

(16) The density probability function curve was obtained by fitting the data to the following formula found in ref 15:

$$P(r_i) = 2r_i/r_0^2 \exp \left\{ - (r_i/r_0)^2 \right\} \text{ where } r_0 = (2/\sqrt{\pi}) r_{av}$$

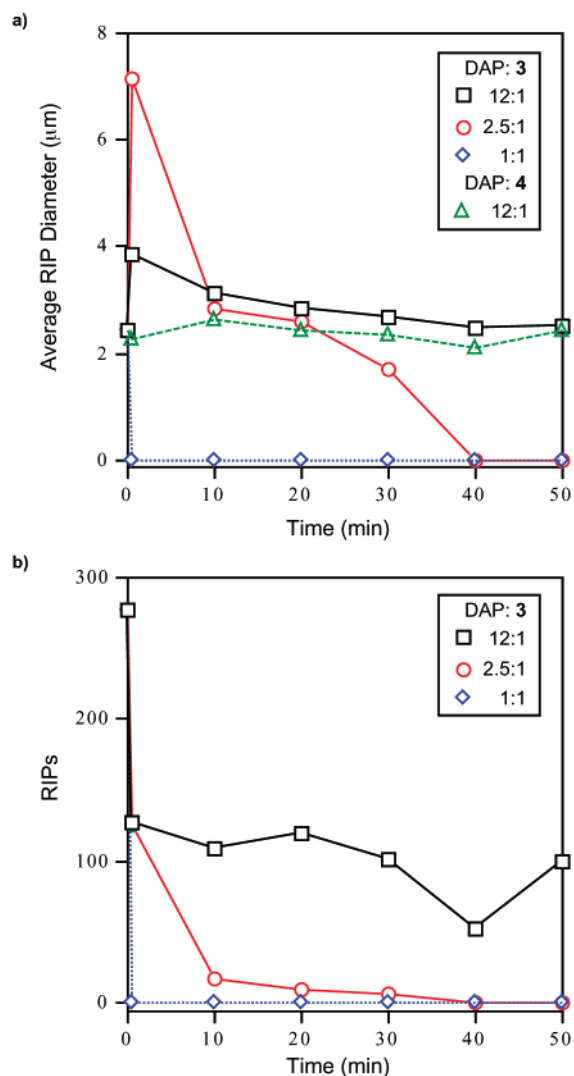


**Figure 4.** (a) Average RIP diameter versus time after addition of **3**, showing initial RIP swelling and subsequent contraction upon addition of **3** over 50 min. Addition of the highly analogous guest **4** does not effect RIP diameter. Incorporation data for diaminopyridine-to-flavin ratios greater than 2.5:1 do not proceed past 40 min as vesicles were completely disrupted (b) Number of RIPs observed in 20 randomly selected DIC micrographs after flavin addition, showing complete disruption of vesicles at higher guest concentrations.

functionality of **3** competitively binds with the diaminopyridine sites within the vesicle wall. This weakens the walls of the vesicles, resulting in the temporary increase in RIP diameter. Over time vesicle disruption occurs, with concomitant release of the polymer components. The fact that both vesicle size and size distribution return to values similar to those of the original polymersomes strongly suggests that relatively little flavin is incorporated into the equilibrated RIPs.<sup>17</sup>

Multivalent guests would be expected to interact very differently with RIPs due to their ability to form multiple contacts with functionality present in the vesicle walls. This hypothesis was tested through the interaction of the multivalent nanoparticle guest **Thy-Au** (~10 thymine units/nanoparticle) with RIPs in DAP:Thy ratios ranging from 25:1 to 450:1 RIP to **Thy-Au** (5 mg/mL in CHCl<sub>3</sub>) solutions. In previous investigations, we have shown that **Thy-Au** interacts with

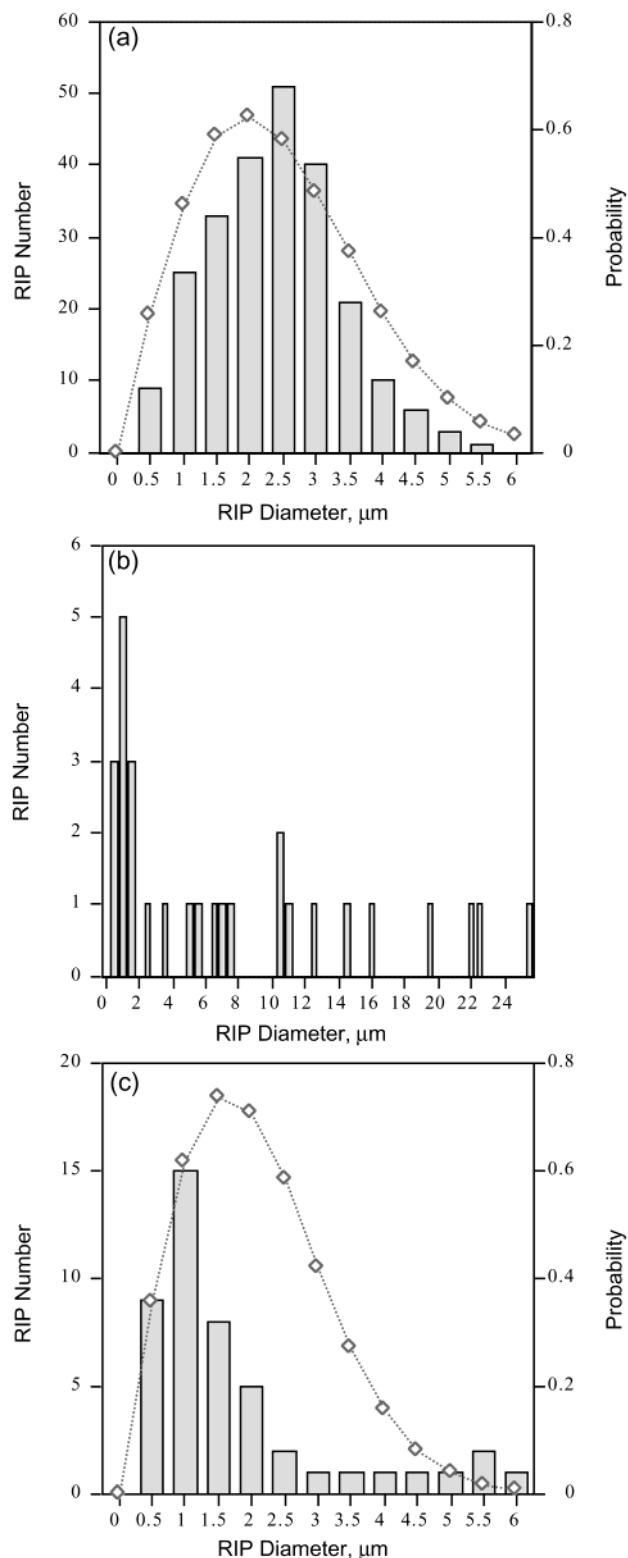


**Figure 5.** (a) Size distribution and an overlay of probability function of initial, undoped RIPs ( $t = 0$  min). (b) size distribution of RIPs 10 min after addition of **3** (12:1 DAP:3) showing wide range of observed diameters as well as dramatic increase in polydispersity of RIPs. (c) RIP distribution 40 min after addition of **3**. Over this time, the RIP system equilibrates to a distribution similar but somewhat smaller than prior to guest addition.

polymers analogous to polymer **1** to form solid spherical assemblies.<sup>18</sup> From these studies, we can predict that **Thy-Au**

(17) Efforts to observe flavin in the vesicle using fluorescence microscopy were unsuccessful due to high background levels of flavin **3**.

(18) Boal, A. K.; Ilhan, F.; DeRouchey, J. E.; Thurn-Albrecht, T.; Russell, T. P.; Rotello, V. M. *Nature* **2000**, *404*, 746–748.

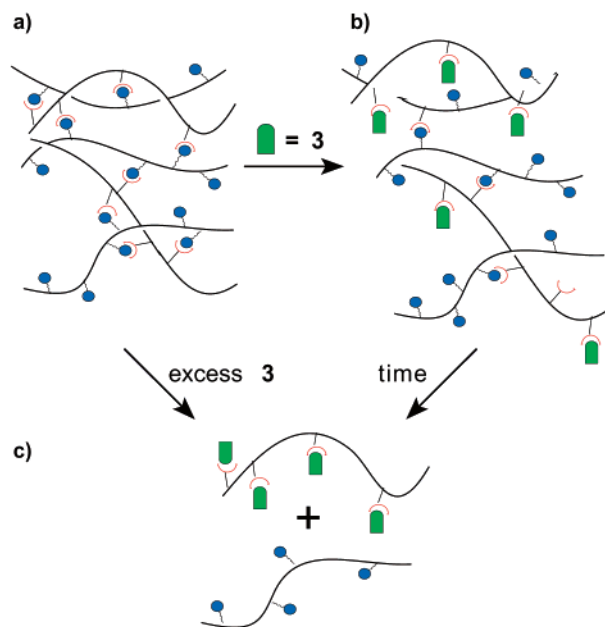


**Figure 6.** Schematic of the proposed mechanism of RIP disruption by flavin **3** (a) interstrand hydrogen bonding prior to addition of **3**, (b) RIP swelling due to competitive binding by flavin **3**, and (c) dissociated polymer strands.

would specifically incorporate into the RIP wall due to favorable multivalent interactions, with excess **Thy-Au** causing a major reorganization of the vesicle morphology.

Time-lapse DIC experiments were performed over a period of 60 min to monitor and quantify the observed morphology changes that occur upon addition of **Thy-Au** (Figure 7). DIC micrographs taken immediately after the addition of **Thy-Au** show a progressive incorporation of nanoparticles into the vesicle wall over a 10 s period. Prior to addition of **Thy-Au**, the spherical RIPs are translucent as a consequence of light traversing through the vesicle (Figure 7a). Immediately after the addition of **Thy-Au**, the overall solution turned dark, followed by very rapid clearing (<5 s) with concomitant darkening of the RIPs arising from **Thy-Au** incorporation into the vesicle structure (Figure 7b). Extended time-lapse data show the average RIP diameter to decrease immediately upon incorporation of **Thy-Au**. The rate of this contraction is concentration-dependent: the most concentrated solution produces the most rapid decrease in average diameter. Interestingly, the RIPs doped with different concentrations of **Thy-Au** develop into a more monodisperse population, as well as equilibrate over a period of 60 min to approximately the same diameter ( $\sim 1 \mu\text{m}$ ). This size is at the limits of observation using optical microscopy, suggesting that many of the aggregates are on the nanometer scale. This conjecture was substantiated by using Transmission Electron Microscopy (TEM) to visualize the structures resulting 60 min after RIP doping (Figures 8). From the micrographs obtained, a size distribution was generated clearly indicating that most structures are submicron scale (Figure 9). Last, to ensure that **Thy-Au** uptake and the resulting RIP morphology changes were specific, we added **MeThy-Au**, the N-alkylated analogue of **Thy-Au**. After repeating the DIC studies, the solution remained dark indicating that no incorporation had occurred (Figure 7d). This demonstrates a “lock-and key” regulated uptake mechanism, reminiscent of cellular uptake of peptide-tagged exogenous materials.<sup>19</sup>

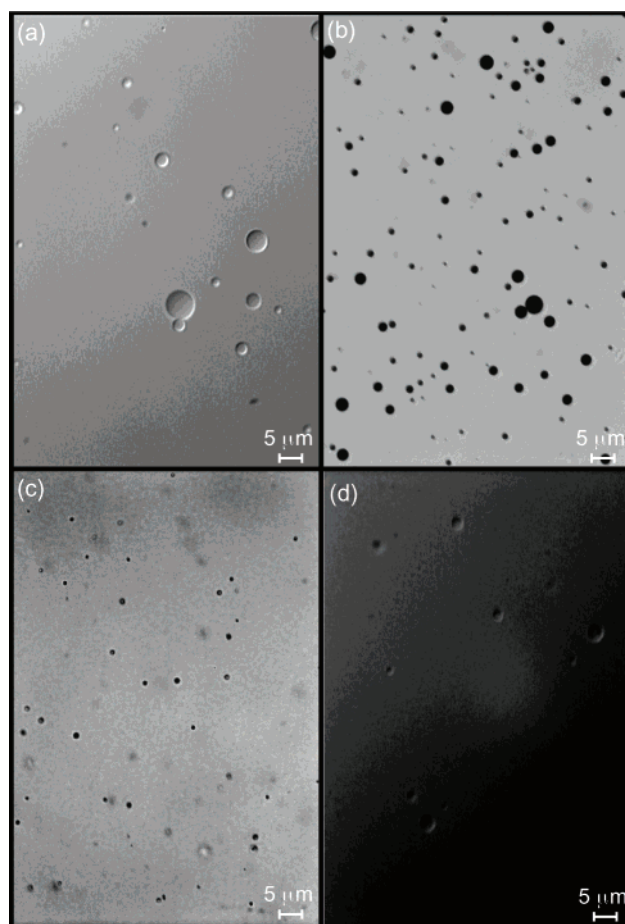


**Figure 7.** (a) 1–2 RIPs only; (b) doped RIPs resulting from combination of a 100:1 DAP:Thy ratio; (c) new self-assembled spherical aggregates obtained after adding excess **Thy-Au** resulting in a 40:1 DAP:Thy ratio; and (d) dark RIP solution after introduction of **MeThy-Au** indicating specific uptake.

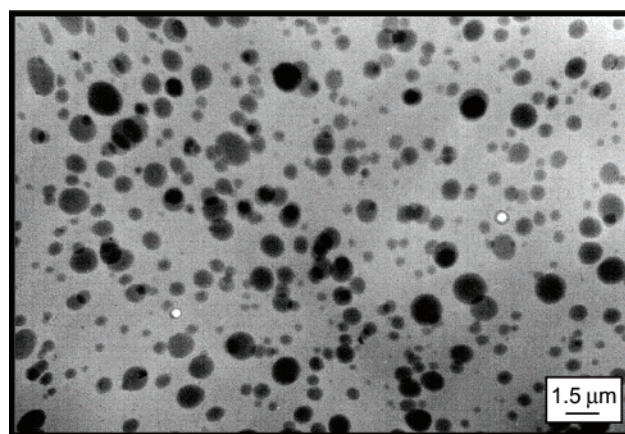


**Figure 8.** Transmission Electron Micrographs of **Thy-Au** doped RIPs (corresponding to a 140:1 DAP:Thy ratio), 60 min after combination.<sup>20</sup>

In addition to the structures observed, new smaller self-assembled spherical structures were obtained upon adding a large excess of **Thy-Au** (Figure 10) to the initial RIP-nano-

(19) Lindgren, M.; Hallbrink, M.; Prochiantz, A.; Langel, U. *Trends Pharm. Sci.* **2000**, *21*, 99–103. Garipey, J.; Kawamura, K. *Trends Biotech.* **2001**, *19*, 21–28. Singh, D.; Bisland, S. K.; Kawamura, K.; Garipey, J. *Bioconjugate Chem.* **1999**, *10*, 745–754. Morris, M. C.; Chaloin, L.; Heitz, F.; Divita, G. *Curr. Opin. Biotech.* **2000**, *11*, 461–466.

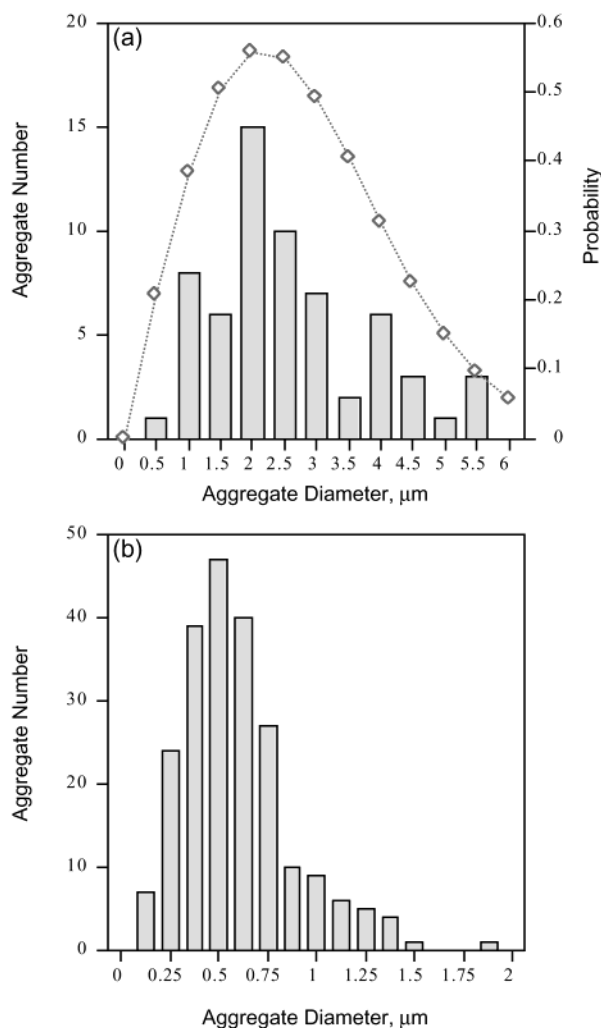


**Figure 9.** Size distributions of: (a) initial solution of RIPs with an overlay of the probability histogram, and (b) resulting spherical aggregates 60 min after combination of RIP solution and **Thy-Au** (140:1 DAP:Thy).<sup>20,21</sup> Data were not fit with probability histogram as there is no evidence for vesicular structure in these rearranged systems.

particle conjugate (Figure 7c). This change in morphology was reversible: addition of polymer **1**: polymer **2** RIP solution resulted in rapid restoration of the native vesicle structures.

## Conclusions

In summary, we have demonstrated the recognition-specific interaction of guests with RIPs. In the case of monovalent guests, these interactions disrupt the vesicle structure. This ability to control vesicle stability provides a mechanism for controlled release of materials incorporated within the vesicle, with applications in a variety of areas, including drug delivery and coating and materials. With multivalent guests, specific uptake of appropriately functionalized guests was achieved, with concomitant control of RIP size and morphology. This selective incorporation of tagged systems provides a starting point for the engineering of highly complex membranes featuring “lock and key” specificity.

(20) Doped RIPs depicted in Figure 7 have been dropcast onto a TEM grid. This creates a flattening effect making the aggregates appear slightly larger than they normally are in solution.

(21) Because the resulting spherical aggregates cannot be conclusively determined to be vesicles, no effort was made to fit the aggregates to a probability function.

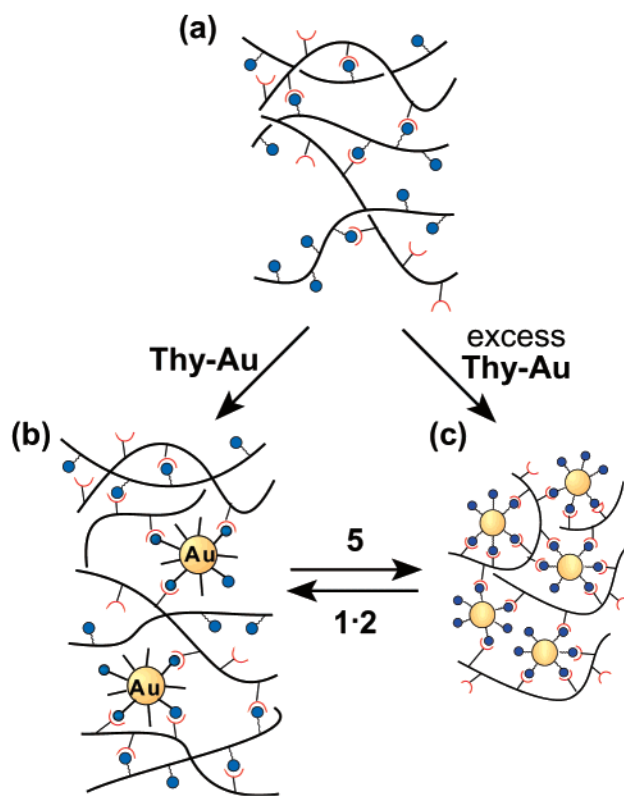


**Figure 10.** Schematic illustration showing proposed structures of: (a) interstrand interactions between polymers **1**:**2**; (b) **Thy-Au** doped vesicle; (c) polymer strand reorganization occurring after addition of excess **Thy-Au**.

## Experimental Section

All chemicals were of reagent grade and were used without further purification unless otherwise noted. All solvents used were of spectroscopic grade and were stored over molecular sieves prior to use.

**Preparation of RIPs.** RIPs were prepared by mixing together 3 mg/mL solutions of polymers **1** and **2** in  $\text{CHCl}_3$ . These samples were then allowed to equilibrate at room temperature for no less than 1 h before experimentation.

**Sealed glass slide apparatus.** Microscope slides were prepared by drilling a 15 mm hole centered on a  $1 \times 75 \times 50$  mm glass slide. A 22 mm square no. 1 cover slip was then affixed to the slide with epoxy, covering the drilled hole. Covering with a second coverslip created a seal preventing evaporation of chloroform during the time lapse studies.

**Flavin Incorporation.** Three different concentrations of flavin **4** were prepared (0.1, 0.5, and 1 mg) and placed in separate vials. Prior to microscope study, 1 mL of RIP solution was added to the flavin-containing vials (to give concentrations of 0.1, 0.5, and 1.0 mg/mL) and gently shaken. The resulting samples provide DAP:flavin molar ratios of 12:1, 2.5:1, and 1:1, respectively. Small aliquots were removed from vial every 10 min for microscope study.

**Thy-Au Incorporation.** A solution of 5 mg/mL in  $\text{CHCl}_3$  **Thy-Au** was prepared and used as a stock solution. In quantitative studies, 4 samples were prepared in separate vials: 19:1, 9:1, 6:1, and 4:1 RIP solution to **Thy-Au** solution. These samples correspond to DAP:Thy molar ratios of 450:1, 220:1, 140:1, 100:1, respectively. Small aliquots were removed from each vial every 10 min for microscope study.

**Acknowledgment.** This research was supported by the National Science Foundation (DMR-9809365, MRSEC) and (CHE-0213554). V.M.R. acknowledges support from the Alfred P. Sloan Foundation, Research Corporation, and the Camille and Henry Dreyfus Foundation.

**Supporting Information Available:** Additional histograms for flavin **3-** and **Thy-Au**-doped assemblies (PDF). This material is available free of charge via the Internet at <http://pubs.acs.org>.

JA026418+